Blazar Variability Workshop II: Entering the GLAST Era
ASP Conference Series, Vol. 350, 2006
H. R. Miller, K. Marshall, J. R. Webb, and M. F. Aller

Jets Kinematics of AGNs at High Radio Frequencies

Svetlana G. Jorstad and Alan P. Marscher
Institute for Astrophysical Research, Boston University, 725 Commonwealth Ave., Boston, MA 02215

Matthew L. Lister
Department of Physics, Purdue University, 525 Northwestern Ave., West Lafayette, IN 47907-2036

Alastair M. Stirling
University of Manchester, Jodrell Bank Observatory, Macclesfield, Cheshire, SK11 9DL, UK

Timothy V. Cawthorne
Center for Astrophysics, University of Central Lancashire, Preston, PR1 2HE, UK

José L. Gómez
Insituto de Astrofísica de Andalucía (CSIC), Apartado 3004, Granada 18080, Spain

Walter K. Gear
School of Physics and Astronomy, Cardiff University, 5, The Parade Cardiff CF2 3YB, Wales, UK

Jason A. Stevens and E. Ian Robson
Astronomy Technology Centre, Royal Observatory, Blackford Hill, Edinburgh EH9 3HJ, UK

Paul S. Smith
Steward Observatory, University of Arizona, Tucson, AZ 85721

James R. Forster
Hat Creek Observatory, University of California, Berkeley, 42231 Bidwell Rd. Hatcreek, CA 96040

Abstract. We have completed a 3 yr program of polarization monitoring of 15 active galactic nuclei with the Very Long Baseline Array at 7 mm wavelength. At some epochs the images are accompanied by nearly simultaneous polarization measurements at 3 mm, 1.35/0.85 mm, and optical wavelengths. We determine apparent velocities in the jets of all sources in the sample. We suggest a new method to estimate Doppler factor of the jet components based on their VLBI properties. This allows us to derive the Lorentz factors and viewing angles of superluminal knots and opening angles of the jets. The Lorentz factors of the

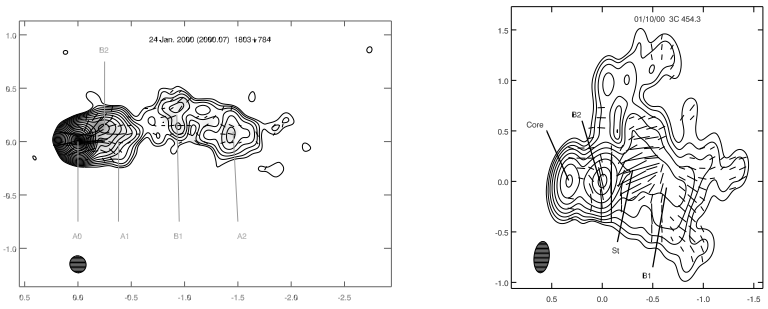

Figure 1. Total (contours) and polarized intensity images of the BL Lac object 1803+784 and the quasar 3C 454.3. The line segments indicate polarization intensity and direction of electric vectors.

jet flows in the different blazars range from $\Gamma \sim 5$ to 40. The quasars in our sample have similar opening angles and marginally smaller viewing angles than the BL Lacs. The radio galaxies have lower Lorentz factors and wider viewing angles than the blazars.

1. Introduction

We have obtained total and polarized intensity images of 8 quasars (0420−014, 0528+134, 3C 273, 3C 279, PKS1510−089, 3C 345, CTA102, 3C 454.3), 5 BL Lac objects (3C 66A, OJ 287, 1803+784, 1823+568, BL Lac) and 2 radio galaxies (3C 111, 3C 120) with the Very Long Baseline Array (VLBA) at 7 mm (43 GHz) at 17 epochs from 1998 March to 2001 April. Figure 1 presents examples of the images for two sources. The VLBA observations are accompanied at many epochs by nearly simultaneous (within two weeks) measurements of polarization at 1.35/0.85 mm (230/350 GHz) and at optical wavelengths. In the second half of the program simultaneous polarization observations at 3 mm were performed at several epochs. The main goals of the project are to relate emission regions at high frequencies to the parsec-scale jet structure and to investigate the strength, direction, and variability of the magnetic field close to the central engine. These can be achieved only after detailed investigation of the jet kinematics. This paper presents some results of the analysis of the jet structure and its variability associated with ejection and propagation of disturbances down the jet based on the VLBI data that we collected over 3 yr. The complete version of the study is given in Jorstad et al. (2005).

Studying the jet kinematics involves many aspects of jet physics. Observationally, the critical parameters of the jet are Lorentz factor, angle between the jet axis and the line of sight, and Doppler factor. These can be derived for superluminal sources from VLBI data and total flux monitoring. A widely applied method to estimate Lorentz and Doppler factors from VLBI data uses the *fastest* feature in the jet by assuming that such apparent velocity should be representive of the true flow velocity and the viewing angle is then taken to be $\Theta_\circ \sim \sin^{-1}(1/\beta_{\rm app})$, where $\beta_{\rm app}$ is the apparent speed of the fastest feature

(e.g., Vermeulen & Cohen 1994). Another way of deriving the Doppler factor is to compare the X-ray flux with the synchrotron flux density of the region of the source which is suspected to be producing the X-rays via the self-Compton process (Marscher 1987). A third way of estimating the Doppler factor using VLBI data is to compute the ratio between observed brightness temperature, $T_{\rm b,VLBI}$ (e.g., Kellermann et al. 1998) and intrinsic brightness temperature, $T_{\rm b,int}$. Readhead (1994) suggests that the maximum intrinsic brightness temperature for powerful synchrotron radio sources does not change significantly from source to source and equals the equipartition brightness temperature, $T_{\rm eq} \sim 5 \times 10^{10}$K. One more way of calculating the Doppler factor, proposed by Lähteenmäki & Valtaoja (1999), uses the variability brightness temperature derived from total flux variations and timescale of the variability. Lähteenmäki & Valtaoja (1999) argue that $\delta_{\rm var}$ is more accurate then the other estimates of Doppler factors and especially important for deriving the Lorentz factor and viewing angle when the total flux variability is represented by flares associated with ejections of superluminal components.

We offer a new method of estimating the Doppler factors of superluminal radio sources based on intensive VLBI monitoring at high radio frequencies that allows sampling of the light curve of a superluminal component close to the VLBI core.

2. Apparent Speeds in Parsec Scale Jets

We find superluminal apparent speeds for 19 of 22 components in the two radio galaxies, 19 of 31 knots in the five BL Lac objects, and 46 of 53 knots in the eight quasars. Figure 2 (*left panel*) presents the distributions of the apparent speeds of all identified components in the jets. An inhomogeneous Friedmann-Lemaître-Robertson-Walker cosmology, with $\Omega_m = 0.3$, $\Omega_\Lambda = 0.7$, and Hubble constant $H_\circ$=70 km s^{-1} Mpc^{-1} (Kantowski, Kao, & Thomas 2000), is adopted for the calculations. Figure 2 shows that more than 50% of the quasar components have apparent speeds faster than 10c. Athough the distribution for knots in BL Lacs covers a wide range of the apparent speeds from -2 to 28c (a negative apparent speed implies motion upstream), it peaks at jet velocities with low negative proper motion. The latter is most likely the result of brightness fluctuations of stationary diffuse features or position oscillations of quasi-stationary knots. This phenomenon is reported also in the results from the 2-cm survey (Kellermann et al. 2004). The two radio galaxies, which have "blazar-like" radio properties, display relatively stable apparent speed, 3-5c, for many detected knots.

According to the χ^2 test, one component in the radio galaxy 3C 120, five components in two BL Lac objects, and 13 components in six quasars exhibit a statistically significant change in the proper motion with time corresponding to acceleration/deceleration with distance from the core. Therefore, in 9 out of 15 sources the apparent speed of individual components varies. For each non-ballistic component, we compare the instantaneous apparent speed at different distances from the core with the average apparent speed, and assign a value representing the apparent speed at each angular distance of $+1$ if the velocity is higher than the average, -1 if it is lower than the average, and 0 if it equals the average. Then we construct the distribution of such changes along the jet (Fig. 2, *right panel*). The distribution shows that an increase of apparent speed with

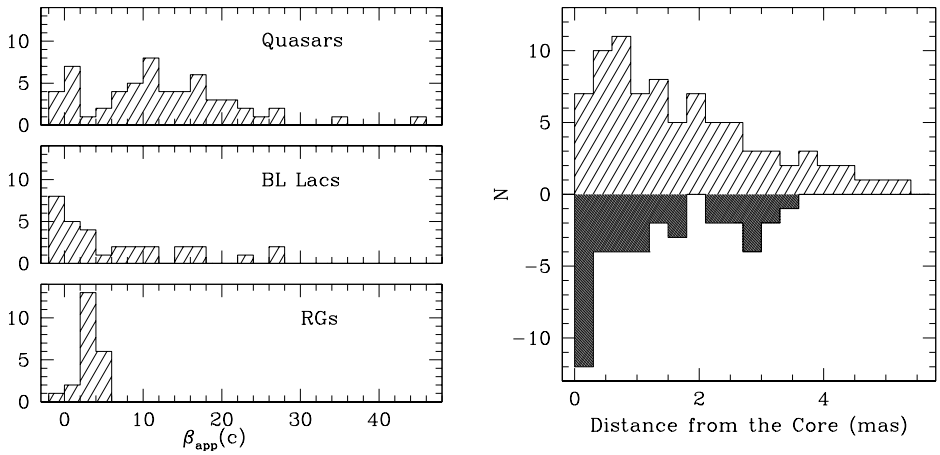

Figure 2. *Left panel*: Distribution of apparent speeds of the jet knots. *Right panel:* Distribution of the instantaneous apparent speed relative to the average apparent speed as a function of distance from the core.

distance from the core is observed at least a factor of 2 times more frequently than the opposite case. The cause of the accelerations could be bending combined with selection of objects with high Doppler factors such that the mean angle to the line of sight of the region near the core is less than optimal for superluminal motion. Statistically, such jets are more likely to bend away from the line of sight, thus increasing their apparent speeds with distance from the core. Alternatively, the acceleration could be physical, caused by considerably higher energy density in relativistic particles than in rest mass (Daly & Marscher 1988) or magnetic acceleration (Vlahakis & Königl 2004).

3. Physical Parameters of the Jet Components

We construct the light curve for each superluminal component using the flux density measurements from the VLBA images. An example of the light curve for the superluminal knot B2 in the jet of the quasar 3C 454.3 (see Fig. 1) is shown in Figure 3 (*left panel*). This allows us to define the timescales of the variability as $\Delta t_{\rm var} = dt/ln(S_{\rm max}/S_{\rm min})$, where $S_{\rm max}$ and $S_{\rm min}$ are the measured maximum and minimum flux densities, respectively, and dt is the time between $S_{\rm max}$ and $S_{\rm min}$. If we assume that the variability timescale corresponds to the light-travel time across the knot, then the variability Doppler factor can be derived as $\delta_{\rm var} = \frac{s\ D}{c\ \Delta t_{\rm var}\ (1+z)}$, where D is the luminosity distance, s is the angular size of the component, equal to $1.6a$ for a Gaussian with FWHM=a measured at the epoch of maximum flux if the true geometry is similar to a uniform face-on disk. We demonstrate (Jorstad et al. 2005) that at high radio frequencies this assumption is most likely correct.

We estimate the projected half opening angle, $\theta_{\rm p}$, for each source using the ratio between apparent transverse size, $s_{\rm t}$, of the jet and apparent longitudinal distance, $s_{\rm l}$, of components: $\theta_{\rm p} = \tan^{-1}\ \psi$, where ψ is the slope of the best linear fit to the relation between $s_{\rm t}$ and $s_{\rm l}$ as defined at the position of each

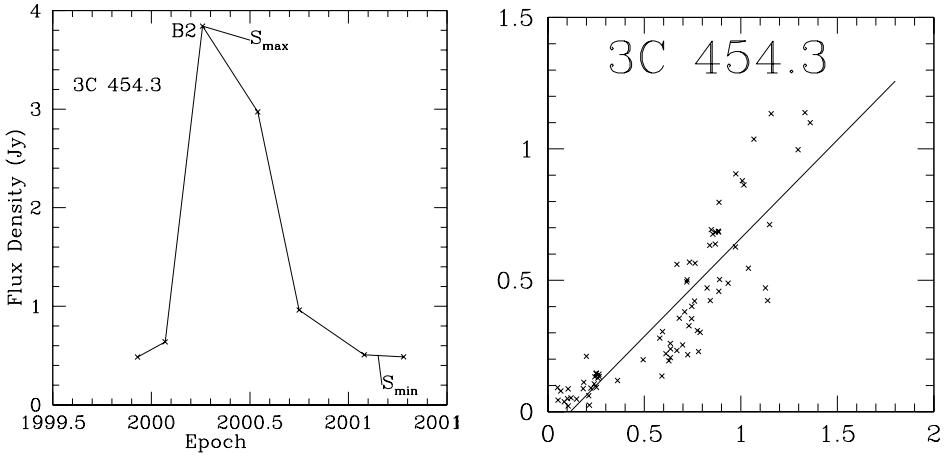

Figure 3. *Left panel:* The light curve of the superluminal knot in the quasar 3C 454.3. *Right panel:* Projected transverse size of the jet vs. longitudinal distance from the core in mas. The solid line repesents the best linear fit to the data.

component that is brighter than 1% of the peak intensity. The values of $s_{\rm t}$ and $s_{\rm l}$ are calculated as follows: $s_{\rm l} = R$, where R is the observed separation of the component from the core; and $s_{\rm t} = R\ \sin\ (|\Theta_{\rm jet} - \Theta|) + a/2$, where $\Theta_{\rm jet}$ is the projected direction of the jet as defined by the mean position angle of all sufficiently bright components over all epochs, Θ is the position angle of the component, and a is the size of the component. Figure 3 (*right panel*) shows the obtained relationship between $s_{\rm t}$ and $s_{\rm l}$ for the quasar 3C 454.3.

Measurements of the apparent speed and estimates of the Doppler factor allow us to calculate the Lorentz factor, Γ, viewing angle, $\Theta_\circ$, and intrinsic brightness temperature for 43 knots in the quasars, 19 knots in the BL Lacs, and 15 knots in the radio galaxies. There is a significant correlation between $1/\Gamma$ and $\Theta_\circ$ (coefficient of correlation 0.83, Fig. 4, *left panel*) expected in flux limited samples (Lister & Marscher 1997). We calculate the values of $< \delta >$, $< \Gamma >$, and $< \Theta_\circ >$ for different subclasses of AGNs averaging the values for individual components with weights inversely proportional to the uncertainty in apparent speed. We use the average viewing angles to estimate the intrinsic half opening angle, θ, for each jet as $\theta = \theta_{\rm p}\ \sin < \Theta_\circ >$. In Figure 4 (*right panel*), the estimated half opening angles are plotted versus the derived Lorentz factors. There is an obvious decrease of θ toward higher values of Γ that agrees with the expectation of standard models of relativistic jets that the opening angle of the jet should be inversely proportional to the Lorentz factor (e.g., Blandford & Königl 1979).

Although each subclass has a large scatter around the average values and statistically the difference in the parameters of the quasars and BL Lac objects is negligible, the points form a continuous sequence on a 3-D plot of δ, $\Theta_\circ$, θ with: quasars ($< \delta >$=23±11, $< \Theta_\circ >$=2.6°±1.9°, θ=0.5°±0.3°) $\longrightarrow$ BL Lacs ($< \delta >$=13.5±6.7, $< \Theta_\circ >$=4.4°±3.0°, θ=0.6°±0.4°) $\longrightarrow$ radio galaxies ($< \delta >$=2.8±0.9, $< \Theta_\circ >$=19.5°±3.2°, θ=3.2°±0.5°). Since our sample is not a complete one, the major differences suggested by these results need to be investigated further with larger, complete samples.

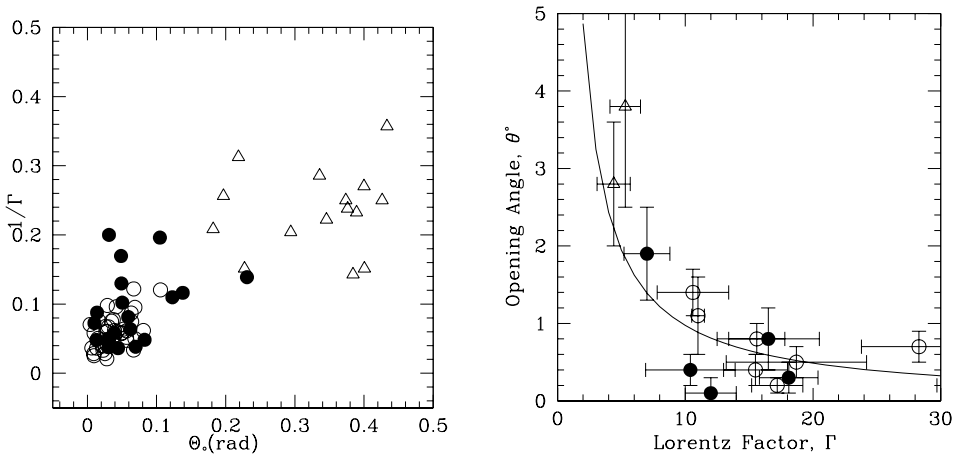

Figure 4. *Left panel*: Inverse Lorentz factor vs. viewing angle for superluminal jet components in the quasars (open circles), BL Lac objects (filled circles), and radio galaxies (triangle). *Right panel:* Half opening angle vs. Lorentz factor of the jets. The solid curve corresponds to the best approximation according to the χ^2 test of the *observed* dependence within the assumed law $\theta = \rho/\Gamma$, where ρ is a constant.

Acknowledgments. This material is based on work supported by the National Science Foundation under grants no. AST-0098579 and AST-0406865. The VLBA is a facility of the National Radio Astronomy Observatory, operated by Associated Universities Inc. under cooperative agreement with the National Science Foundation.

References

Blandford, R. D. & Königl, A. 1979, ApJ, 232, 34
Daly, R. A. & Marscher, A. P. 1988, ApJ, 334, 539
Jorstad, S. G., et al. 2005 submitted to AJ
Kantowski, R., Kao, J. K., & Thomas, R. C. 2000, ApJ, 545, 549
Kellermann, K. I., et al. 2004, ApJ, 609, 539
Kellermann, K. I., Vermeulen, R. C., Zensus, J. A., & Cohen, M. H. 1998, AJ, 115, 1295
Lähteenmäki, A. & Valtaoja, E. 1999, ApJ, 521, 493
Lister, M. L. & Marscher, A. P. 1997, ApJ, 476, 572
Marscher, A. P. 1987, in *Superluminal Radio Sources*, eds. J.A. Zensus & T.J. Pearson, Cambridge Uni.Press, 280
Readhead, A. C. S. 1994, ApJ, 426, 51
Vermeulen, R. C. & Cohen, M. H. 1994, ApJ, 430, 467
Vlahakis, N. & Königl, A. 2004, ApJ, 605, 656